R. & M. No. 3273

MINISTRY OF AVIATION

AERONAUTICAL RESEARCH COUNCIL
REPORTS AND MEMORANDA

The Performance of Supersonic Turbine Nozzles

By B. S. STRATFORD and G. E. SANSOME

LONDON: HER MAJESTY'S STATIONERY OFFICE
1962
PRICE: 14*s.* 0*d.* NET

The Performance of Supersonic Turbine Nozzles

By B. S. Stratford and G. E. Sansome

Communicated by the Deputy Controller Aircraft (Research and Development), Ministry of Aviation

*Reports and Memoranda No. 3273**
June, 1959

Summary. An investigation has been conducted at the National Gas Turbine Establishment into the performance of turbines having high pressure ratios per stage. The present Report discusses the mode of operation of supersonic nozzles for such turbines, and describes a cascade experiment. Both theory and experiment demonstrate that the conditions imposed upon the supersonic flow immediately downstream of the nozzles (*e.g.*, by a following row of rotor blades) exert an overriding influence upon the nozzle outlet flow angle, and hence upon the maximum pressure ratio obtainable across the nozzle—providing that the axial component of velocity is subsonic. This is an important difference from the more familiar flow of subsonic turbine nozzles, where, for example, the downstream gas angle is controlled predominantly by the nozzle blade shape and spacing. A suitable test technique using a closed-jet tunnel is demonstrated.

The particular nozzles tested, of convergent-divergent form, had a straight-sided divergent portion of $16\frac{1}{2}$ deg total angle, a blade outlet angle of 76 deg (relative to axial direction) and a design Mach number of $2\frac{1}{2}$. The flow was found to be well behaved as regards shock pattern, losses, and starting over the range of pressure ratios tested—between 9/1 and 19/1. In particular the efficiency at the design pressure ratio of 16·6/1 was high, the velocity coefficient calculated from traverses of pitot and static tubes being 0·98.

For the conversion of pitot to total pressure at a Mach number of 2·5 a high accuracy is important in the measurement of the static pressure; nevertheless readings from a conventional four-hole instrument appear to be reliable.

1. *Introduction.* With the advent of the rocket and study of the turbo-rocket, interest has increased in turbines of high pressure ratio, as previously used in, for example, the Curtis and the De Laval steam turbines. The purpose of such turbines is usually to achieve a high work output per stage, while an associated advantage is the ability to use steam or gas of initially high temperature and pressure without obtaining either a large end thrust from the disc face or high temperatures in the main structure of the turbine. These advantages amount in practice to low weight, low capital cost, and simplicity. However, the efficiency that could be expected from high pressure-ratio turbines has not hitherto exceeded 50 to 60 per cent—discussion with the main designers of steam turbines and a perusal of some of the standard works[1, 2] suggest these values—and consequently it is uncommon for such turbine stages employed in modern steam practice to have pressure ratios much in excess of 4/1, except in auxiliary equipment. If the efficiency of substantially higher pressure-ratio stages could be raised to exceed 70 per cent their application both for flight and in steam practice would become more attractive. With this in view, an investigation of the performance of a high pressure-ratio turbine was initiated at the N.G.T.E.

* Previously issued as N.G.T.E. Report No. R.234.—A.R.C. 21,261.

The present Report describes tests on a two-dimensional nozzle cascade having a design based on the nozzle of the first turbine[3] in the N.G.T.E. programme. This turbine is a velocity compounded Curtis stage having a pressure ratio of 22/1 and a design Mach number from the nozzles of 2·4; details of the design are based upon what seemed the best steam-turbine practice.

The value 2·4 for the nozzle Mach number is intermediate in the whole field of supersonic turbines. It is, for example, much higher than would be used in a Curtis wheel forming the first stage of a large steam turbine, where a Mach number of 1·5 would be considered high; on the other hand it is less than for some De Laval nozzles, which appear to have been used up to pressure ratios corresponding to a Mach number of about 4·0 (Ref. 2) and equally it will be less than for a Curtis wheel when used as an auxiliary and subject to the full pressure ratio of the steam plant. The present Mach number is typical of what might be used in the turbines for pure rockets or turbo-rockets. If, of course, pressure compounding of the turbine stages were used in place of velocity compounding, or some reaction incorporated, the nozzle row would no longer have the full pressure ratio across it and its Mach number would be correspondingly reduced.

A great body of research has been carried out on turbine nozzles, extending back many years. The present work endeavours to apply current techniques in aerodynamics to an old problem. Thus, whereas previous tests on nozzle rows, as reported, for example, in Refs. 1, 2 and 4 to 7, have used open-jet tunnels, the present test uses a closed jet, as this is considered to simulate more closely the conditions in the turbine—unless lap is used in the turbine. Also, by preventing mixing at the edges of the jet, the closed-jet tunnel allows a clearer examination of the flow structure and, in addition, it allows checking of the mechanism whereby conditions downstream of a supersonic nozzle row can determine the static pressure and gas angle at the exit from the nozzle. The flow pattern is examined with the aid of Schlieren pictures, further details of the flow behaviour being provided by traverses for the pitot and static pressures. The velocity coefficient is obtained from the traverses, this method again differing from most previous nozzle testing where, except for some recent Russian work[7] about which few details are available, the velocity coefficient has been based upon a measurement of the mass flow and either the reaction from the jet, or its impulse, upon a plate placed in its path.

The mode of operation of supersonic cascades, and the testing technique required to obtain a range of cascade pressure ratios in a closed-jet tunnel, are considered in a preliminary discussion in Section 2.

2. *Preliminary Discussion of the Flow Behaviour in Supersonic Cascades, and of Test Techniques.* Considerable theoretical and experimental work has been carried out on the mode of operation of cascades for transonic and supersonic compressors and for transonic turbines, as for example in Ref. 7 to 11. In the discussion which follows, some of the results of this work will be applied to supersonic turbines, and it will be demonstrated that:

(1) Whereas for subsonic nozzle rows the gas exit angle is determined by the cascade geometry almost independently of the downstream static pressure, for supersonic rows the gas exit angle is controlled by the downstream static pressure provided the axial component of velocity is subsonic.

(2) The incidence on to the following row of turbine rotor blades is determined uniquely by the shape and thickness of the rotor-blade leading edge, at a given inlet Mach number, and

cannot be arbitrarily prescribed by velocity triangles. Ordinarily this incidence would be small and positive, the theoretical value becoming zero when the thickness of the blade leading edge is zero.

(3) In a turbine it is the determination by the rotor of its own incidence which would be expected to control the gas angle and static pressure at the nozzle exit.

(4) For a closed-jet cascade tunnel the gas angle and static pressure may be varied for the whole of the cascade exit by varying the angle of one downstream wall of the tunnel. This wall simulates the effect of the leading edges of the next blade row in the turbine.

2.1. *The Shock Pattern at the Nozzle Exit.* For simplicity an inviscid flow is considered in an infinite cascade of isentropic nozzles, the latter having trailing edges of zero thickness and wedge angle as in Fig. 1. One possible mode of operation for such a cascade is with the gas exit angle equal to the angle of the nozzle passage centre-line at the trailing edge. There is no shock system at the blade trailing edges and the static pressure at exit is just that which would be calculated taking the exit area to be in the plane T_1B, *i.e.*, normal to the direction of the nozzle exit flow.

For most turbine nozzles it seems likely that the axial component of velocity will be subsonic and when this condition holds, a second mode of operation is possible, as shown in Fig. 2. Since the component of velocity perpendicular to any Mach line is always sonic, whereas the axial component of velocity is subsonic, a shock wave from one trailing edge, say T_1, will be incident as shown on the blade surface upstream of the next trailing edge T_2 and, with its reflection, will cause a double increment of pressure rise in the flow along the surface BC. Now the static pressures in the two flows from C and D on either side of the trailing edge T_2 must equalise at the trailing edge and so the flows will deviate there, such that that from C passes through a Prandtl-Meyer expansion while that from D passes through a shock. Moreover, if the deviation which causes the shock at T_1 was of magnitude δ' the deviation at T_2 will be seen to be δ' also, in order that the pressures may equalize; consequently a shock system generated in some way at T_1 will be propagated without diminution successively from blade to blade along the cascade. Downstream the shock system will become attenuated, and from considerations of momentum and continuity it follows as in Appendix I that the final conditions downstream will, to a first order, and for weak shocks, be equal to the mean conditions across the pitch in the plane of the trailing edges. (For example if the reflected shock E F intersects T_1T_2 a distance d from T_1, d being readily calculable from the shock-wave angle, the final deviation δ will be related to δ' by $\delta \doteqdot (d/s)\delta'$, s being the pitch of the blades.) The final gas angle will be related to the final static pressure, still supposing the shock system to be weak, by the usual isentropic flow relations between pressure ratio and area ratio. For the area ratio in the present flow, the throat area is that of the passage design, while the effective outlet area is $s \cos(\beta_0 + \delta)$, the gas angle being $(\beta_0 + \delta)$. The relationship is of course independent of the details of the exit shock system, the latter merely providing the mechanism whereby these quantities may be varied from downstream while the nozzle blades remain fixed. (Examples of this control from downstream will be given in Sections 2.2 and 2.5 for the turbine and the tunnel respectively.)

Thus for supersonic nozzle rows having the axial component of velocity subsonic the final fluid exit angle is a function of the downstream static pressure rather than being fixed by the cascade geometry. If a change of downstream pressure is imposed upon the cascade there will be a change in the exit shock pattern and a corresponding change in fluid outlet angle.

2.2. *Rotor Incidence and its Effect on the Nozzle Flow.* If an infinite cascade of flat blades of zero thickness is placed in the uniform flow well downstream of the nozzles it will necessarily operate at zero incidence. One explanation of this phenomenon is as follows. Whatever the incidence occurring at any one leading edge, say L_1 in Fig. 3, the flow downstream of the shock or expansion wave springing from L_1 will be parallel to the blade L_1A. Now the leading edge L_2 of the adjacent blade is downstream of this wave (the axial Mach number being subsonic) and the adjacent blade is therefore at zero incidence to the local flow. However, both the cascade and the oncoming flow are uniform so that the local incidences must all be equal. This is possible only if the local incidences are all zero. There is then no shock system, and the incidence relative to the upstream flow is zero.

Since the cascade of thin blades determines its own fluid inlet angle, it determines also the fluid outlet angle for the nozzles. The mechanism whereby this is brought about becomes clearer on considering a small change in the stagger angle of the downstream cascade of thin blades. On making such a change each blade would tend to produce a shock or expansion wave momentarily at its leading edge. When this wave has extended far enough from the leading edge, the incidence of the adjacent blade will be reduced to zero and hence all the waves will stop forming. However, the momentarily formed portions of wave would unite to form a pitchwise wave front which would travel axially upstream (at the speed of sound relative to the axially-subsonic flow) until it reached the nozzle exit region, where the pressure change across it would generate a new shock pattern to yield the requisite static pressure and flow angle. A similar sequence would occur in practice whenever a turbine rotor changed speed, the nozzle gas outlet angle changing to match the incidence requirement of the rotor during the change in operating conditions.

In practical turbines the rotor blades may have a chamfered leading edge of moderate thickness and then the incoming flow passes through a shock system such as sketched in Fig. 4. As has become realised during the last few years the unique operating incidence, measured relative to the flat upper surface of the blade, is not zero for thick leading edges but has some small positive value, typically in the region of 3 deg; the method of calculation and a physical reason why only one incidence is possible are given in Appendix II. With thick leading edges it is this unique positive incidence which would be expected to determine the nozzle outlet angle.

With the cascade of rotor blades having thick leading edges situated immediately downstream of the nozzle cascade, the nozzle and rotor shock systems will overlap, and will also be reflected from the various blade faces. Moreover, for a nozzle cascade having a non-isentropic expansion from the throat, as for example in the commonly used straight divergent type, the nozzle exit flow will have superposed upon it the shock pattern produced by the main expansion. The overlap and reflection would cause variations in the flow exit angle from blade to blade along the nozzle row and similar variations of incidence from blade to blade along the rotor row. Such effects are probably very difficult to analyse and it will be assumed that experience will indicate whether such variations can unduly affect performance. In the meantime it would appear desirable to reduce the variations to a minimum; to this end one would endeavour to use both thin rotor-blade leading edges and thin nozzle trailing edges, having small chamfer and wedge angles; the angle of the camber-line at the nozzle trailing edge would probably be made about equal to the required gas outlet angle, while the passage shape would be contoured so as to minimise the development of shock waves. The flow variations would not, however, be expected to alter the general conclusion that the rotor cascade will determine both its own mean operating incidence and the mean gas exit angle from the nozzle. Tests mentioned in Section 2.4 lend support to this argument.

2.3. *Lap.* The conclusion of the previous section is modified for a turbine with 'lap'; in such a turbine the nozzle exit flow discharges into an annulus having a sudden enlargement. If the increase in area is great the rotor flow would be bounded by a region of dead air which might act as a by-pass through which the back pressure applied from downstream could reach the nozzles. It would be expected that the nozzle outlet angle and static pressure would then be determined by the combined effect of the rotor leading edge and the static pressure of the dead-air region, the relative influence of these two factors depending, it would seem, upon the distance between the sudden expansion and the plane of the rotor leading edge. This type of turbine is not considered in any detail in the present discussion, even though it has certain advantages. The insertion of lap causes a gross flow separation at the annulus wall, whereas it is the aim in most aerodynamic machines to avoid flow separation. Cascade tests[12] have confirmed that lap is likely to cause serious losses; consequently it is assumed that a turbine which is designed to give as high an efficiency as is compatible with a high pressure ratio will not use lap and that the nozzle exit flow is bounded at the ends of its span by the annulus walls.

2.4. *Another Possible Interaction between the Nozzle and the Rotor Cascades.* In the preceding discussion of the flow through two successive cascades it has been assumed that fully expanded supersonic flow had been established through both blade rows. As discussed in Ref. 3, however, if the losses either within the second blade row or at its entry, were greater than had been assumed in the blade design there would be a danger of choking, the system becoming 'locked' with a mixed supersonic and subsonic flow in the nozzles and a sonic flow at some position in the rotor. Subsequent to the present investigation a few tests have been made in which the present nozzle cascade was followed by a multi-bladed row of impulse blades (of similar design to that adopted in the turbine described in Ref. 3). These tests showed that fully expanded supersonic flow could be established; they also gave qualitative confirmation of the arguments of Section 2.2, but appeared to indicate that the boundary layer on the walls at the end of the span also affected the interaction between the two cascades.

2.5. *Tunnel Design.* In a tunnel test on a cascade of nozzle blades the basic aim is to determine the behaviour of the flow under conditions simulating those of the turbine. Now for subsonic cascades the outlet angle is determined uniquely by the cascade geometry, and so the requirement from the tunnel is to have an unrestricted outlet—*i.e.*, an open-jet tunnel—so that the flow may take up its true angle. Also, as the aspect ratio of the blades is usually fairly large it is deemed adequate to measure only the two-dimensional losses in the cascade and to estimate end losses semi-theoretically or empirically; thus the mixing of the open jet at the ends of the span is not important. For the high pressure-ratio turbine, however, the aspect ratio of the blades is usually low and it is desirable to include the end losses in the tunnel measurement. This requires end walls in the traverse region downstream of the cascade (*i.e.*, going at least part way towards a closed-jet tunnel) in order that the end boundary layers are properly simulated and so that the pressure distribution does not degenerate to a constant pressure at the ends of the span. Moreover, with supersonic cascades the desirability of keeping both noise level and power consumption to a minimum favours a closed-jet tunnel. This type of tunnel also facilitates flow photography—provided Perspex or glass end walls are practicable—by maintaining conditions more uniform across the span and by eliminating the interference from mixing at the jet edges. Thus there are strong reasons for favouring a closed-jet tunnel and it remains only to decide whether the static pressure at the cascade exit can be controlled in such a tunnel.

With the closed-jet tunnel the pressure level when the flow is fully supersonic may be varied only by varying the geometry, so that the tunnel scheme shown in Figs. 5 and 6 has been used for the tests of the present Report. The feature relevant to the immediate discussion is a set of interchangeable blocks which provided a range of angles for the wedge face AB. If there were no complications such as reflections from this face the various shock patterns corresponding to Fig. 2 should be reproduced by changing simply the angle of AB. Thus the basic behaviour of the cascade would be as indicated in the sketches of Fig. 7. The shock or expansion wave from A would be incident on the next blade and would be propagated along the cascade as described in Section 2.1, the flow angle and static pressure downstream of this shock changing in each passage with each change in block angle. Subsequent sections of this Report show the extent to which this holds and the extent to which reflections from the face AB complicate the interpretation. It is to be noted that changing the angle of the other side wall of the tunnel at exit would have no effect on the cascade as the latter is not in the Mach cone of influence from the beginning of that wall. There would also be no virtue in having both side walls adjustable unless there were embarrassments from area changes in the duct downstream of the cascade.

An alternative configuration for the tunnel might be to retain closed walls downstream at the ends of the span, but to leave AB open so that the boundary angle of the flow along AB would adjust itself to suit an imposed static pressure. This would seem to show little practical advantage and several disadvantages, of which probably the most important is that with such a large swirl angle β_0 the mixing of moving and stationary gas at the interface would spread across and obscure much of the flow field. Reflections from the face would still occur, with the difference that compression waves would be reflected as expansion waves and *vice versa*.

2.6. *Definitions of Velocity Coefficient.* In work on impulse turbines the performance of a blade row is usually represented by its 'velocity coefficient', *i.e.*, the ratio of the mean gas velocity at exit, to the velocity if the flow were isentropic. The representation is very convenient as the efficiency of such turbines may be expressed directly in terms of the velocity coefficients for the various blade rows, independently of Mach number and pressure ratio. When quoting a measurement for velocity coefficient, however, there is a difficulty in deciding how the mean velocity should be defined.

The mean velocity could be defined as a mass-flow mean (sometimes referred to as a momentum mean) or as an area mean, the velocity being determined at each point in the exit plane and hence the mean found. Alternatively, the measured total pressure could be averaged in the exit plane —again either as a mass mean or as an area mean—and the mean velocity taken to be that which would correspond to the mean total pressure. In the earlier experiments on blading for steam turbines the cascade performance was obtained from measured values of the mass flow, together with either the reaction force on the blade row, or the impulse force on a plate placed perpendicular to, and in, the exit jet. This gives the momentum mean, the reaction or impulse force being equal to the momentum flux in the jet. The momentum mean is just

$$\bar{V} = \int V dm / \int dm$$

where dm is an element of mass flow, and is therefore a mass-flow mean of velocity. In the present experiments on the other hand, measurements are made of the distribution of total pressure in the exit plane and the simplest computational procedure is to use a velocity based on the area mean of total pressure; the relation between velocity coefficient and total-pressure coefficient (the latter

defined as the ratio of the total pressure at exit to that at inlet) when the isentropic Mach number is 2·50, is shown in Fig. 8, the derivation being discussed briefly in Appendix III. In the present Report the result is quoted both as a velocity based on the area mean of total pressure and as a momentum mean. Although in extreme instances the values resulting from these two definitions could differ widely, they have been found to yield closely the same result for the typical profiles tested in the present programme.

Workers in the U.S.A. often employ a mass mean of total pressure. This gives a true measure of the energy flux at the measuring station, but it therefore makes no allowance for either the mixing losses occurring downstream or the adverse effect of a maldistribution upon subsequent blade rows, and so would be expected to lead to an optimistic estimate of performance. Analysis of the flow in a parallel duct indicates that the area mean total pressure before the mixing would be somewhat less than the true total pressure after; thus the area-mean might be taken as a more reasonable measure of the performance after allowing for both the mixing loss which occurs downstream and the adverse effect of the maldistribution on subsequent blade rows.

3.0. *Apparatus.* The cascade tunnel, constructed of wood and Perspex, is shown in the sketch of Fig. 5 and in the photograph of Fig. 6. Smooth conditions were obtained at entry to the cascade by means of gauzes and a honeycomb, followed by a settling length and a 4/1 contraction. (The profile for the final part of the contraction was the cubic $y = x^3/15b^2$, where b is the width of the working section, x the distance upstream, and $(y + b/2)$ the distance of either wall from the centre-line of the contraction.) The tunnel received air at about room temperature dried to a nominal dew-point of − 80 deg C and supplied at a gauge pressure of a few inches of water.

The cascade had two blades (made of aluminium) and three passages, the blade design being taken from the mean-diameter section of the nozzle for the first turbine[3] in the N.G.T.E. programme. Details of the design are shown in Fig. 9. The aspect ratio was the same as in the turbine and the scale 1·56 times as large, giving a span of 1·25 in. The various nozzle angles were as follows:

Passage centre-line angle	76 deg
Camber-line angle at the trailing edge	72 deg
Design gas angle	74 deg
Expansion total included angle	16½ deg

Since the tunnel cascade, unlike the turbine, did not have fillets in the throat at the ends of the span, the geometrical area ratio was appreciably smaller than in the turbine. Inspection of the passages gave the following values for the area ratio, the exit area being measured perpendicular to the passage centre-line.

Upper passage	2·57/1
Middle passage	2·66/1
Lower passage (adjacent to face AB)	2·58/1
Mean	2·60/1
(Nominal design	2·75/1)
(Turbine design	3·08/1)

The values were consistent to about $\pm$ 1 per cent for the two possible builds, *i.e.*, with the clear Perspex wall (for photography) in position or an alternative wall with static tappings. The free-stream Reynolds number at the design condition was $1{\cdot}6 \times 10^6$ based on chord, or $0{\cdot}8 \times 10^5$ based on throat width. For comparison, the turbine Reynolds number based on chord would be $3{\cdot}6 \times 10^6$.

The exit from the cascade was enclosed for the reasons discussed in Section 2.5. The set of blocks allowed the angle of the face AB to be changed in two-degree steps from 80 deg to 72 deg. The end walls of the working section were in $\frac{1}{2}$ in. Perspex; compared with plate glass, this facilitated the design of the tunnel using the end walls as structural and locating members. However, although Perspex gave a simple tunnel design and a cheap Schlieren system which could be easily interpreted by visual examination on the test bed, it is not ideal for photography. When looking at the relevant Figures (10, 15 and 18) care must be taken to differentiate between shock waves and marks from the Perspex. As for ordinary supersonic wind tunnels the working section was followed by an almost parallel mixing section in which a normal shock is assumed to occur, the mixing section leading to a short subsonic diffuser. Suction was provided by a Holland exhauster.

The pitchwise distribution of static pressure along one end wall was measured by static tappings placed on a line $\frac{1}{8}$ in. axially downstream of the plane of the trailing edges. Pitot and static traverses could be made in the exit flow, further details being given in Section 4.0 and Appendix IV. (The large pitot instrument which may be seen in the photograph of the tunnel was not used, it being unsuitable for traverses other than at mid-span.)

Schlieren photographs were taken at three pitchwise positions in order to cover the 12 in. wide field of interest, composite pictures being prepared.

4.0. *Results and Discussion.* Traverses and photographs of the flow are shown in Figs. 10 to 17, Figs. 10 to 14 giving the results for the nominal design condition—*i.e.*, with the 74 deg block—while the variation with block angle is represented in Figs. 15 to 17. All the Schlieren photographs were taken with the knife edge about parallel to the passage centre-line.

4.1. *Discussion.* A Schlieren photograph of the flow for the 74 deg block is shown in Fig. 10. It will be seen that the flow, as would be expected, is quite well behaved in that there are no severe shock-wave boundary-layer interactions or other sources of gross loss. (The black marks, one just before the throat of the middle passage and one nearly half way along the 76 deg wall, are due to stresses in the Perspex at the blade location points.)

Wake and boundary-layer traverses are shown in Figs. 11 to 13. The wake traverses were made an inch downstream of the upper trailing edge in the plane marked on Fig. 10 as a white dotted line, the traversing being perpendicular to the flow rather than pitchwise and carried out at six spanwise stations. The boundary-layer traverse was made spanwise at mid-pitch in the central passage, at the point in the plane of the trailing edges marked with a cross in Fig. 10. The traverses shown are for a $\frac{1}{2}$ mm o.d. pitot tube, slightly chamfered at the nose, and for a four-hole $1\frac{1}{2}$ mm o.d. static tube; a further discussion of the instrumentation is given in Appendix IV.

The mean total pressure at each spanwise position is plotted against spanwise position in Fig. 14, the curve being drawn through the points from the wake traverses at mid-span while the boundary-layer traverse is used as a guide near the wall; from this the velocity coefficient based on area-mean total pressure for the whole flow is computed to be 0·983. The corresponding velocity coefficient for the central core of two-dimensional flow (Fig. 11) is 0·993. When defined as a momentum mean, *i.e.*, a mass mean of velocity, the velocity coefficients become 0·985 and 0·991 for the overall

and two-dimensional core respectively. These calculations all neglect the slight loss of momentum resulting from the local gas angle differing from the mean (the loss which corresponds to the divergence loss of conical propelling nozzles), but analysis suggests the corresponding reduction in velocity coefficient would be less than $\frac{1}{2}$ per cent. Thus a final value of 0·98 may be adopted. Expressing the performance in terms of efficiency, *i.e.*, the ratio of the actual kinetic energy at the nozzle exit to the isentropic kinetic energy for the same mass flow, gives a value of approximately 96 per cent.

Typical velocity coefficients obtained in tests on steam-turbine nozzles range between 0·96 and 0·97 (Refs. 1, 2, 4), (although there is appreciable scatter and a few results have been obtained as high as 0·99). Several factors probably help to explain the higher value now obtained. The basic design of the present blade[3] appears to be good. The supersonic expansion is double sided, *i.e.*, symmetrical about the nozzle centre-line, and is sufficiently rapid to give only a short length for boundary-layer growth while being sufficiently gradual to cause only weak shocks (the shock losses in the mainstream contribute only about one-tenth, or less, of the whole loss, while shock/boundary-layer interaction does not appear from the photographs to be significant). Furthermore the trailing edges have been kept very thin in order to reduce wake losses. As regards the details of the testing, the surfaces of the present cascade have been polished to be aerodynamically smooth; care has been taken to obtain a uniform entry flow of reasonably low turbulence, while condensation and any associated losses have been avoided by using dry air. In the open-jet tests on steam nozzles a small loss of momentum would be expected from the mixing on the edges of the jet, as a slight suction force would be induced on the rearward face of the cascade structure[13]. The closed-jet tunnel eliminates this difficulty.

The present velocity coefficient is as high as the values quoted in Ref. 14 for subsonic gas-turbine nozzles of 60 deg outlet angle and moderate aspect ratio, while it is appreciably higher than the values suggested for subsonic nozzles of large outlet angle and small aspect ratio. Part of the improvement is probably due to the fact that most of the turning in the present cascade is accomplished at very low velocities; some of the improvement may also result from the rather idealistic velocity profile at inlet in the present tests.

Comparison may also be made with supersonic propelling nozzles for aircraft. For axi-symmetric nozzles at a Mach number of $2\frac{1}{2}$ the model tests of Ref. 15 give velocity coefficients of about 0·985 to 0·99, for Reynolds numbers of thirty to forty times as high as in the present tests. The comparison seems very reasonable as the propelling nozzle does not have the oblique exit of the turbine nozzle and, therefore, requires only about a half of the wetted area of supersonic flow.

Schlieren photographs for the range of block angles are shown in Fig. 15. It is immediately apparent that there is a progressive change in shock pattern with change in block angle, the change being basically the same for all the passages. As the block angle increases from 72 deg to 80 deg the shock at the beginning of the block wedge intensifies. This effect is propagated in turn to the second and third passages, the shocks from the trailing edges—corresponding to that from the beginning of the block wedge—likewise intensifying. Moreover the angles of the wake—which may be used to give a rough indication of the local flow direction—increase with increase in block angle. Thus in Fig. 16 are plotted the wake angles measured close to each of the two trailing edges, the angles being measured from the originals of the photographs. Although the angles can be given only roughly, it is evident that the wake angles do change by about the same amount as the change in block angle.

In most instances Fig. 15 does not show the expansion fans radiating from the trailing edges as illustrated in Fig. 7. In the latter figure the expansion surfaces of the blades are isentropic, whereas the blades of Fig. 15 have straight divergent passages with a resultant non-zero wedge angle at the trailing edge. The wedge angle causes two shocks in the downstream flow rather than one shock and one expansion fan, except when the turning at the trailing edge is large, as for the 80 deg block angle. From Fig. 16, a 2 deg expansion fan would be expected on the lower side of the blades for the 80 deg block angle, as the blade surface is at 76 deg (Fig. 9) while the wake is plotted at 78 deg. There is in fact some evidence of an expansion fan, particularly for the right-hand blade, but the expansion is followed by a shock. The latter's presence probably results from the behaviour of δ^*, the displacement thickness, in the wake, while the expansion fan is probably stronger than it should be also because of the wake effect. With the 78 deg block angle the nett turning for the lower flow should be zero but again there is a slight expansion present—rather less than for the 80 deg block. It would be reasonable to suppose that the expansion and shock on the lower surfaces for the 78 deg block provide equal and opposite turning, while for the 80 deg block the nett result is a 2 deg expansion.

It will be noticed that there is an appreciable amount of interference from reflections from the block wall—particularly at the larger angles (78 and 80 deg), where the flow is farthest from design. Thus with the 80 deg block a local separation in the second passage nearly half way along the 76 deg wall seems to be due to the convergence of the main-pattern shock with a reflected shock. Also the sinusoidal undulations of the wakes for the 78 and 80 deg blocks may probably be associated with reflections from the block face. However, for flow conditions near design these reflections do not appear to unduly affect the flow and, in particular, the loss measurements at design should be reliable.

Fig. 17 shows the distributions of static pressure across the pitch in a plane $\frac{1}{8}$ in. axially downstream of the trailing edges, the positions of the tappings being marked in Fig. 10. For block angles of 72 to 76 deg, *i.e.*, near the design condition, the pressure would appear reasonably uniform (a standard of judgment is lacking but almost certainly the uniformity of a wind tunnel is not necessary), whereas away from design the pressure variations become considerable. The general level of pressure falls with decrease of outlet angle, all three passages changing together so that the pressure remains about the same in all the passages at any given block angle. This is according to expectation. The pressure ratio for the design condition, *i.e.*, with the 74 deg block, is seen from Fig. 17 to be 16·6/1, the free-stream Mach number then being 2·47; the mean Mach number—as calculated from the velocity coefficient of 0·98—would be 2·38. The range of pressure ratio covered by the tests is from 9/1 to 19/1.

It will be seen from the Schlieren photograph for the 80 deg block, in Fig. 15, that the passage still runs full even when the pressure ratio has been reduced to a little more than half the design value and that at that condition the only boundary-layer separation is quite localised.

The evidence from the photographs and from the distributions of static pressure confirms the general concept of the theory of the trailing-edge shock pattern as explained in Section 2.1 and it shows that the main features of the shock pattern may be reproduced in a closed-jet tunnel in which the outlet static pressure and gas angle are controlled by the variable wedge-angle technique. It seems likely that the flow in a turbine would show a behaviour similar to that of the tunnel, the nozzle outlet conditions being determined by the unique operating incidence of the rotor leading edges. This has, in fact, been demonstrated in subsequent turbine tests in the current programme[3]. In the tunnel the reflections from the variable wall do not appear to influence the results unduly,

and when the deviation of the gas angle from the blade angle is small these reflections may probably be neglected.

The tunnel tests would seem to indicate that the exit flow at the design condition is reasonably uniform, but in a turbine, where the patterns and reflections will be more complicated, it may be desirable to reduce the wedge angle at the nozzle trailing edge in order to keep to a minimum the shock strengths and angle variations in the flow approaching the rotor. The best nozzle design might follow the profile of the shortest fully isentropic nozzle (*i.e.*, containing no shock waves), except on the upper blade surface just before the trailing edge, where the isentropic form, which would require a zero wedge angle at the trailing edge, would be replaced by a straight taper of minimum practicable angle. The deviation of the exit flow should also be carefully considered as discussed in Sections 2.1 and 2.2, the design exit flow being placed along say the camber-line, after allowance for incidence on the rotor. For real blades—with a non-zero wedge angle at the nozzle trailing edge and thickness at the rotor leading edge—the effect would be to design the nozzles for a smaller supersonic expansion within the passages, the expansion being completed in the field of the trailing edges, with a further expansion within the field of the rotor leading edges. The latter expansion is not strictly a part of the nozzle expansion as it occurs in a rotating pressure field and therefore does not alter the velocity which enters into the velocity triangles. One might decide, however, to transfer a part of the nozzle expansion to the field of the rotor leading edges and accept the slight change in the velocity triangles, in order to prevent subsequent recompression within the nominally impulse rotor. Since the geometrical expansion in the nozzles would then be considerably smaller in both area and length the losses might be expected to be less. For a given area ratio within the blade passage, however, it is not to be expected that even a fully isentropic design could give very much improvement over the present velocity coefficient.

An improvement in performance should be obtained if the aspect ratio of the nozzle passage could be increased, as would result if more blades could be used in the annulus with the same annulus height and pitch/chord ratio. Apart from the direct improvement in the nozzles, an indirect improvement would be expected from reduced secondary flow in the rotor as a result of the thinner annulus boundary layer—as discussed in Ref. 12. A limit to the number of blades is likely to be set by the pressure loading, the manufacture of the slender trailing edges and the accuracy of the passage areas.

4.2. *Design Rules.* In designing a supersonic nozzle for a given pressure ratio it is necessary to add to the exit area calculated for an isentropic flow for that pressure ratio, an allowance for the losses. Now if the mean exit angle were assumed to be 73·5 deg in the test with the 74 deg block —variation between the various passages make a close estimate difficult—the geometric exit area would be found to exceed the isentropic area corresponding to the measured pressure ratio of 16·6/1 by nearly 20 per cent. This result, however, is sensitive both to the assumed exit angle and to small errors in static pressure, 1 deg change in exit angle reducing the 20 per cent to 13 per cent and a change in static pressure equal to $\frac{1}{4}$ per cent of the dynamic head making a further reduction to 10 per cent. The present experiment is therefore unsuitable for prescribing a design rule.

In the design method used by Johnston[3] the allowance is calculated by assuming that the losses occur between the throat and the final exit flow and are uniformly distributed in the exit flow; for a velocity coefficient of 0·98 as measured in the present experiment the allowance would become 7 per cent. By comparison with the previous paragraph it would seem that provided the correct velocity coefficient is known, the Johnston method would probably not over-estimate the area

required—the experiment unfortunately is not able to be more helpful than this—and so a design based on that method would have some margin in hand on pressure ratio. This tends to confirm that the design method is a suitable one—at least for nozzles, in which there is no danger of the losses causing unintentional choking. The method would only apply of course if the supersonic part of the nozzle were sufficiently long for all the losses to be assumed to occur there.

5.0. *Additional Tests.* The main tests just discussed were carried out with conditions as close to ideal as could be obtained. Several additional tests concern the behaviour of the nozzles under other conditions.

In a special test with the tunnel aspirating damp (atmospheric) air, the only change indicated by the shock pattern—the 74 deg block was in position—was a very slight reduction of Mach number. In a second test, also using the 74 deg block, a diamond section strip was extended pitchwise at mid-span just downstream of the trailing edges and gave a blockage of 9 per cent. The tunnel still started and produced fully supersonic flow; this was at a slightly lower Mach number than without the blockage, the change being comparable with that produced by a 2 deg change in block angle. The nozzles do not seem particularly sensitive, therefore, to blockage downstream.

Some miscellaneous photographs taken with the control valve in the downstream ducting partly closed are shown in Fig. 18. In each nozzle the flow just downstream of the throat can be attached to one wall only, and then the deviation of the discrete jets from the design angle is quite considerable —although probably not sufficient to cause difficulty in, say, establishing fully supersonic flow even when there is another cascade downstream.

In a further test the flow was examined at entry to the nozzles. It appeared from tufts that there was no separation of the flow at or near the leading edges, except possibly for a small region at one end of the span of one blade, where the tuft was rather erratic. (One of the tufts near mid-span reversed when the tunnel exit valve was only slightly open, but pointed forwards at high speeds.) The results of such a test may not apply to the turbine because of the small number of blades in the cascade and because the Reynolds number and the upstream conditions of turbulence and velocity profile are likely to differ.

The outlet conditions for the nozzle have been varied in the present experiments by varying the angle of the tunnel wall AB (Fig. 5). In order to make a comparison with this method a mean pressure ratio of approximately 10/1, *i.e.*, close to the value for the 80 deg block, was obtained across the cascade while using the 74 deg block by adjustment of the tunnel control valve. As would be expected the two passages farthest upstream expanded fully giving the standard flow pattern for the 74 deg block, while the main 'starting' shock system of the tunnel commenced at about the exit of the third passage. In the first two passages the pressure ratio would be about 16·6/1 and in the third, considerably less than 10/1. Such a test arrangement, therefore, does not seem of value, as conditions change between successive passages of the cascade and in no passage are the required conditions obtained. In the turbine it seems probable, from symmetry, that each passage has substantially the same pressure ratio across it and so the variable-block technique which achieves this uniformity is to be preferred.

6.0. *Conclusions.* The set of turbine nozzles tested appears to have satisfactory operating characteristics. The velocity coefficient is 0·98 at the design pressure ratio of 16·6/1 and the flow is reasonably uniform; at a pressure ratio little more than a half of the design value the passages still run full.

The mode of operation of the cascade confirms theoretical expectations. The axial component of velocity being subsonic, the angle and static pressure of the exit flow are not fixed by the cascade itself but may be varied by varying the conditions downstream. In the tunnel an adjustable wall at exit is successful in changing the exit flow simultaneously in all passages; in a turbine it would be expected (provided fully expanded supersonic flow can be established) that the unique operating incidence demanded by the rotor would determine the flow at the nozzle exit. An entirely closed-jet tunnel appears suitable for testing this type of cascade, although the reflections from one of the walls are a complication.

An improvement, particularly in turbine performance, might be obtained by increasing the aspect ratio of the nozzles by using a larger number of relatively short chord blades of the same pitch/chord ratio. The shorter chord would decrease the annulus boundary layer and hence, also, the secondary flow in the rotor. Practical factors limit the number of blades likely to be used. Some further improvement might be obtained in the rotor performance if the flow at the nozzle exit were more perfectly shock free and uniform. To this end the expansion in the nozzles could be contoured to be isentropic, except for the smallest practicable wedge angle at the trailing edge, while the design angle for the gas at exit, calculated after a generous allowance for rotor incidence, might be better directed along the camber-line at the trailing edge. The possible change in gas angle relative to the blade would be obtained, for a given rotor, by increasing the swirl angle of the nozzle passage and decreasing the area ratio between the exit and the throat. The allowance for rotor incidence could be made in the same way—provided a slight change were acceptable in the velocity triangles—so that nozzles designed on these principles would tend to have a smaller geometrical expansion within the nozzle passages than has the present design.

LIST OF SYMBOLS

α_0	Gas outlet angle from nozzles
α_1	Gas inlet angle to rotor
β_0	Blade outlet angle for nozzles
β_1	Blade inlet angle for rotor
C_p	Pressure coefficient (equal to the ratio of any pressure to a datum pressure, in this instance the cascade inlet total pressure)
δ'	Local angle of flow deviation in plane of trailing edge
δ	Angle of flow deviation at infinity
dm	Element of mass flow
d	Distance shown in Fig. 2
M'	Isentropic Mach number
M	Actual mean Mach number
M_∞	Mach number at infinity upstream of a rotor cascade in an infinite field of flow
P_{tot}	Total pressure
P_{pitot}	Pressure as measured directly on a pitot tube (less than total pressure in supersonic flow)
P_{stat}	Static pressure
t	Blade leading-edge thickness
T_{tot}	Total temperature
S	Pitch of blades
V	Local velocity
$\overline{V}$	Mean velocity
V'	Velocity (for Appendix III)
ϕ	Velocity coefficient
y, u, v, p, ρ	Quantities defined in Appendix I

REFERENCES

No.	Author	Title, etc.
1	A. Stodola	*Steam and gas turbines.* Vol. I and II (translated by L. C. Loewenstein, 1927). Peter Smith. New York, 1945.
2	W. J. Kearton	*Steam turbine theory and practice.* Isaac Pitman and Sons, London, 1922 to 48.
3	I. H. Johnston and D. C. Dransfield	The test performance of highly loaded turbine stages designed for high pressure ratio. A.R.C. R. & M. 3242. June, 1959.
4	—	First to sixth reports of the Steam-Nozzles Research Committee of the Institute of Mechanical Engineers. *Proc. Instn. Mech. Engrs.* 1923 to 30.
5	J. H. Keenan	Reaction tests of turbine nozzles for supersonic velocities. *Trans. A.S.M.E.* Vol. 71. pp. 773 to 780. October, 1949.
6	Hans Kraft	Reaction tests of turbine nozzles for subsonic velocities. *Trans. A.S.M.E.* Vol. 71. pp. 781 to 787. October, 1949.
7	M. E. Deich	Flow of gas through turbine lattices. (Translation 'Technical Gasdynamics' (Tekhnickeskaia gazodinamika) ch. 7. 1953). N.A.C.A. Tech. Memo. 1393. May, 1956.
8	A. Kantrowitz	The supersonic axial-flow compressor. N.A.C.A. Report 974. 1950.
9	A. Ferri	Preliminary analysis of axial-flow compressors having supersonic velocity at the entrance of the stator. N.A.C.A. Research Memo. L9G06. TIB/3115. September, 1949.
10	R. Staniforth	On the testing of supersonic compressor cascades. A.R.C. 19,877. September, 1957.
11	C. H. Hauser, H. W. Plohr and G. Sonder.	Study of flow conditions and deflection angle at exit of two-dimensional cascade of turbine rotor blades at critical and supercritical pressure ratios. N.A.C.A. Research Memo. E9K25. TIB/2260. March, 1950.
12	B. S. Stratford and G. E. Sansome	Theory and tunnel tests of rotor blades for supersonic turbines. A.R.C. R. & M. 3275. December, 1960.
13	B. S. Stratford	A further discussion on mixing and the jet flap. *Aeronautical Quarterly.* Vol. III. August, 1956.
14	D. G. Ainley and G. C. R. Mathieson	An examination of the flow and pressure losses in the blade rows of axial flow turbines. A.R.C. R. & M. 2891. March, 1951.

REFERENCES—*continued*

No.	*Author*	*Title, etc.*
15	P. F. Ashwood, G. W. Crosse and Jean E. Goddard.	Measurements of the thrust produced by convergent-divergent nozzles at pressure ratios up to 20. A.R.C. C.P. 326. November, 1956.
16	S. Goldstein (Editor)	*Modern developments in fluid dynamics.* University Press. Vol. I. pp. 248 to 250. 1938.
17	W. F. Cope	The measurement of skin friction in a turbulent boundary layer at a Mach number of 2·5, including the effect of a shock wave. *Proc. Roy. Soc.* A. Vol. 215. p. 84. 1952.
18	D. R. Chapman and R. H. Kester ..	Turbulent boundary-layer and skin-friction measurements in axial flow along cylinders at Mach numbers between 0·5 and 3·6. N.A.C.A. Tech. Note 3097. March, 1954.

APPENDIX I

Conditions where the Exit Wave Pattern has become Attenuated

Let y be the distance measured perpendicular to the axis, u and v velocities parallel and perpendicular respectively to the axis, dm an element of mass flow, p the static pressure and ρ the density. Let suffix $_0$ in this Appendix refer to conditions when the wave pattern has become attenuated.

If the wave pattern is weak the parameters may be expressed:

$$u = u_0 + \delta u, \qquad v = v_0 + \delta v, \quad \text{etc.}, \tag{1}$$

where the δu etc. are small so that powers of δu above the first may be neglected.

The total whirl momentum is constant for all axial stations:

$$\int v dm = \text{const.} = \int v_0 dm. \tag{2}$$

The total mass flow is constant for all axial stations:

$$\int dm = \int \rho u dy = \text{const.} = \int \rho_0 u_0 dy. \tag{3}$$

The fluid obeys the perfect gas laws for adiabatic changes:

$$p/\rho^\gamma = \text{const.}, \qquad \text{i.e., } \delta p = (\gamma p_0/\rho_0)\delta\rho. \tag{4}$$

The flow is isentropic:

$$\delta p + \rho u\, \delta u + \rho v\, \delta v = 0,$$

$$\text{i.e., } \delta p = -(\rho_0 u_0 \delta u + \rho_0 v_0 \delta v). \tag{5}$$

From Equations (1) and (2)

$$\int \delta v dm = 0. \tag{6}$$

Hence,

$$\int \rho u \delta v\, dy = 0, \qquad \int \rho_0 u_0 \delta v\, dy = 0$$

and

$$\int \delta v\, dy = 0. \tag{7}$$

From Equations (1) and (3)

$$\int [\rho_0 \delta u + u_0 \delta\rho] dy = 0 \tag{8}$$

and from Equations (4) and (5)

$$\delta\rho = -(\rho_0/\gamma p_0)(\rho_0 u_0 \delta u + \rho_0 v_0 \delta v). \tag{9}$$

Equations (8) and (9) give:

$$\int [\rho_0 \delta u - (u_0 \rho_0/\gamma p_0)(\rho_0 u_0 \delta u + \rho_0 v_0 \delta v)] dy = 0 \tag{10}$$

and substitution of Equation (7) then gives:

$$\int (\rho_0 - u_0^2 \rho_0^2/\gamma p_0)\delta u dy = 0,$$

i.e.,

$$\int \delta u dy = 0. \tag{11}$$

If f is any function of u and v, Equations (7) and (11) give:

$$\int \delta f dy = \int \left[\left(\frac{\partial f}{\partial u}\right)_0 \delta u + \left(\frac{\partial f}{\partial v}\right)_0 \delta v \right] dy = 0, \tag{12}$$

so that, in particular,

$$\int \delta\alpha dy = 0, \tag{13}$$

where α is the flow angle. Hence, referring to Fig. 2 (where δ is the deviation and not a difference coefficient):

$$\delta = (d/s)\delta' \tag{14}$$

as stated in the text. Also:

$$\int \delta p dy = 0. \tag{15}$$

Thus where the wave pattern has become attenuated all parameters take on their mean values in the plane of the trailing edges. As the variations are supposed to be small, there is no differentiation between area means and mass means.

APPENDIX II

The Calculation of the Incidence on the Subsequent Rotor Cascade and the Physical Reason why there is only One Value Possible for the Incidence

The incidence on the rotor cascade is readily calculated from considerations of continuity when the wedge angle of the leading-edge chamfer is insufficient to cause shock detachment or significant total-pressure loss.

There are two conditions governing the flow.

(1) If the flow angle upstream is α_1, the blade angle β_1, and if t is the leading-edge thickness at the shoulder of the chamfer, the upstream flow area per blade is $s \cos \alpha_1$ and the flow area just inside the blade passage is $(s \cos \beta_1 - t)$. Thus the incoming flow has to expand or compress to take up a change in area per blade of $[(s \cos \beta_1 - t) - s \cos \alpha_1]$, and it has also to turn through the angle $(\alpha_1 - \beta_1)$.

(2) The shock system ahead of the cascade is essentially different from that in passage flow. In the latter, compression (or expansion) and turning can be obtained independently and any combination—within limits—is possible as the flow has a controlling wall on each side of it. In the shock system ahead of the cascade the flow in any stream tube passes through waves which all emanate from surfaces (the leading edges) on one side of it; thus all expansions of flow area are accompanied by turning in one sense and all compressions by turning in the opposite sense, and for any given net turning angle $(\alpha_1 - \beta_1)$ there will be a corresponding net expansion of flow area, defined uniquely by the Prandtl-Meyer solution for flow at a corner. (It would, for example, be impossible to achieve compression without turning.)

Thus the only incidence at which the cascade can operate is that at which the expansion of flow area corresponding to a Prandtl-Meyer turn of magnitude $(\alpha_1 - \beta_1)$ is equal to the expansion geometrically available, *i.e.*, $[(s \cos \beta_1 - t) - s \cos \alpha_1]$. The incidence is thus determined.

The value obtained when $\beta_1 = 70$ deg and $t/(s \cos \beta_1) = 0{\cdot}065$ is $2{\cdot}9$ deg when $M_\infty = 1{\cdot}90$ and $5{\cdot}0$ deg when $M_\infty = 2{\cdot}50$. The corresponding Mach numbers immediately inside the blade passage are $2{\cdot}00$ and $2{\cdot}72$. These values hold if there is a chamfer such that the whole of the thickness t is on the upper side of the chamfer point as in Fig. 4; for say a symmetrical leading edge t would be replaced by $t/2$. If the chamfer angle is large enough for there to be an appreciable loss of total pressure in the entry shock system the incidence is increased, and the calculation then requires a detailed examination of the shock pattern.

APPENDIX III

The Relationship between Velocity Coefficient and Total-Pressure Coefficient—see Section 2.6 and Fig. 8

For the calculation of this relationship the value of $V/\sqrt{T_{tot}}$ is read from tables of compressible flow for each of two values of P_{tot}/P_{stat}—that with P_{tot} equal to the measured outlet total pressure and that with it equal to the isentropic, *i.e.*, the inlet, total pressure; a common value is used for P_{stat}. The value of P_{stat} for nozzle testing may be taken as the mean measured at the exit, although the calculation is not sensitive to the static pressure adopted provided the same value is assumed in the actual flow as in the isentropic. Now the actual total temperature is the same as the isentropic (as the energy dissipation does not alter the total temperature other than by internal heat transfer, which may be assumed negligible in its effect on mean values). Consequently the velocity coefficient is equal simply to the ratio of the two values of $V/\sqrt{T_{tot}}$.

Alternatively the relationship may be deduced from first principles by a method similar to that of Appendix III of Ref. 14, the result being:

$$\frac{P_{tot}}{P_{tot\ inlet}} = \left[1 - \frac{\gamma - 1}{2} M^2 \left(\frac{1}{\phi^2} - 1\right)\right]^{\gamma/(\gamma-1)}$$

or,

$$\frac{P_{tot}}{P_{tot\ inlet}} = \left[1 + \frac{\gamma - 1}{2} (M')^2 (1 - \phi^2)\right]^{-\gamma/(\gamma-1)}$$

where M' is the isentropic Mach number, M the actual mean outlet Mach number and ϕ the velocity coefficient. A useful approximation is:

$$1 - P_{tot}/P_{tot\ inlet} = \gamma M^2(1-\phi) + O(1-\phi)^2$$

or

$$1 - P_{tot}/P_{tot\ inlet} = \gamma (M')^2(1-\phi) + O(1-\phi)^2$$

APPENDIX IV

Conversion of Pitot Pressure to Total Pressure

The pitot pressure readings in the present experiment were converted in the usual way to values of total pressure by means of Rayleigh's formula, this allowing for the loss of total pressure across a normal shock. At Mach numbers in the vicinity of 2·5 the correction is highly sensitive to errors in static pressure. Thus for a given value of pitot pressure a change in static pressure by an amount equal to 10 per cent of the absolute static will change the value predicted for the total pressure by 10 per cent of the total pressure. Also, the dynamic head at a Mach number of 2·5 is sixteen times the absolute static pressure. Now in subsonic flow static pressures are not usually relied upon to much better than 1 per cent of the dynamic head. If the same held for supersonic flow, therefore, we should not expect the corrected total pressures to be reliable to much closer than about 16 per cent at the present test level of Mach number. A 16 per cent error on total pressure would correspond to a 2 per cent error on velocity coefficient (*see* Fig. 8).

In many boundary-layer explorations the effect of the above uncertainty would be reduced when the local values were rendered non-dimensional by dividing by the values in the mainstream, as small errors from the static-pressure measurement would tend to cancel. In the present experiment the calculation of the losses requires a knowledge of the absolute value of the total pressure and an error of even half that suggested above would be unacceptable. Now the losses in the mainstream are effectively just the shock losses; since these are small they may be calculated with adequate accuracy from the Schlieren photographs of the flow pattern and the result used to check the accuracy of the pitot/static conversion. Calculations based on the shock pattern for the flow with the 74 deg block indicate that the average loss of total pressure in the mainstream in the plane of the traverse stations will be between about $\frac{1}{2}$ per cent and $1\frac{1}{2}$ per cent, the exact amount depending upon the rapidity with which the shock waves are attenuated. Thus the measured value for the total pressure in the mainstream should be close to 0·99 of the inlet total pressure. Examination of the traverse results of Figs. 11 to 13 shows that the local values of the corrected total pressure in the mainstream are within 4 per cent of this value and that the average for the mainstream would be much closer. This accuracy is considered adequate. It may be added that the comparison between the corrected total pressures and the values predicted from the calculation of the shock losses implies a very high accuracy in the static pressure when the error is expressed in terms of the dynamic head, a typical error here being appreciably less than $\frac{1}{4}$ per cent of the dynamic head. However, expressed in this way, a high accuracy is, perhaps, to be expected for supersonic flow when the absolute static is such a small proportion of the dynamic head. The static instrument used in the traverses was of the four-hole type, $1\frac{1}{2}$ mm o.d. hypodermic tubing, holes nominally 0·010 in. diameter at a position 0·90 in. from the tip of the nose and 1·00 in. from the rear of the stem, the nose cone having a 10 deg included angle and a smooth fairing at the shoulder. The pitot had a 0·22 in. long nose of $\frac{1}{2}$ mm o.d. hypodermic tubing chamfered at its tip, held *via* lengths of 1 mm and $1\frac{1}{2}$ mm tubing in a $1\frac{1}{2}$ mm stem, the distance from the nose to the rear of the stem being 1·00 in. Having found that this pair of tubes gave an accurate value for total pressure in the mainstream it seemed reasonable to accept as accurate the values measured for the static pressure in the wake and in the boundary layer—especially as in the regions where the losses are large and the Mach number lower the conversion of the pitot pressure becomes much less sensitive to the values of the static. In the boundary-layer traverse it was ascertained that the reading for the static pressure remained steady on approaching the wall, so that any significant wall effect on static pressure was unlikely.

One of the static traverses was repeated using a second instrument in which the four holes were replaced by an annular slot of width 0·010 in., the two parts of the instrument being joined internally across the slot by a triangular prism. This second instrument had become suspect in a previous experiment[12] and was therefore checked in the present experiment where the correct value of the total pressure could be calculated theoretically. The annular instrument was of a fairly well-known type, being mentioned, for example, in Ref. 16. When the tube diameter is small such that the holes of the four-hole instrument become very small the annular instrument may be preferred for ease of manufacture and because of its more rapid response. These advantages did not hold in the present circumstances however, as the manometers used were vertical mercury manometers which gave a negligible time lag with either instrument, while the instrument makers made the four-hole instrument with facility. Moreover, the four-hole static is a fairly robust instrument, in contrast to the annular which is fragile and easily suffers misalignment; thus in practice the annular static was at a disadvantage. The main disadvantage discovered in the present annular instrument, however,

was one which is easily avoided once the situation is appreciated. Across the annulus there was a step down in the external surface of about 0·002 in. (having used stainless steel rod upstream of the slot, in order to obtain a sharp nose, and hypodermic tubing downstream). A Prandtl-Meyer expansion might be expected from the 0·002 in. step, and consequently the pressure in the slot would be less than in the free stream. It is presumed that this was the cause of the error found in the present instrument, the values of total pressure based on its readings being typically 10 per cent high, implying that it was reading low by an amount equal to $\frac{1}{2}$ to $\frac{3}{4}$ per cent of the dynamic head. The difficulty is of course readily overcome, for example by putting the junction between the rod and the tubing at the shoulder of the nose cone, and in the present type of work some such simple precaution to ensure a good surface finish at the slot would be essential. No tests were made on a revised design to check its accuracy. Although the precaution suggested is easily adopted it is concluded that the four-hole static is the more suitable instrument for the present type of work on account of its greater robustness and because a good surface finish is more readily ensured.

No accurate comparison was attempted between the four-hole static tube and the wall statics but their agreement seemed at least reasonable. It will be seen from Fig. 13 that there is a small variation of static pressure between the wall and mid-span and in general it is essential for reliability to use a local rather than a wall static for converting the pitot readings.

In an endeavour to guard against error, all the pitot traverses were repeated with a second instrument, this being of $1\frac{1}{2}$ mm diameter chamfered at the nose, while the pitot traverses in the boundary layer were checked with a third instrument of 1 mm diameter. Also, the wake traverses were made at a position 1 in. downstream of the trailing edge in order that the minimum velocities should be well above sonic and hence the interference small between the normal shock at the nose of the tube and the flow. The mean wake losses were the same for the two traverses, but the distribution across the span was slightly different. The boundary-layer traverses also showed some discrepancies. This is not surprising in view of the scale of the passage, it being accepted that to reduce to a very low level the wall effect of a pitot tube—caused presumably by interaction between the normal shock from the tube and the boundary layer being traversed—the tube diameter should be of the order of 1/40 of the boundary-layer thickness $\delta_{0\cdot99}$ (Refs. 17, 18), which in the present experiment was approximately 0·11 in. However, the value of the boundary-layer loss indicated by the $\frac{1}{2}$ mm probe was equal to the mean of the losses indicated by the other two probes, and was therefore adopted. Judging from the discrepancies found between the various traverses the maximum likely error in the final area-mean pressure coefficient would seem to be appreciably less than 4 per cent, so that the corresponding velocity coefficient as quoted in Section 4.1 should be accurate to better than $\frac{1}{2}$ per cent.

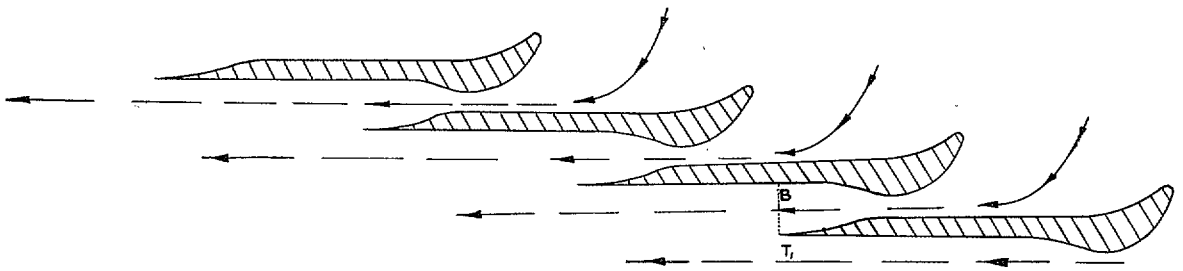

FIG. 1. No shock system at exit and zero deviation of the flow.

$\alpha_o = \beta_o + \delta$

$\delta \doteq \delta' \cdot a/s$

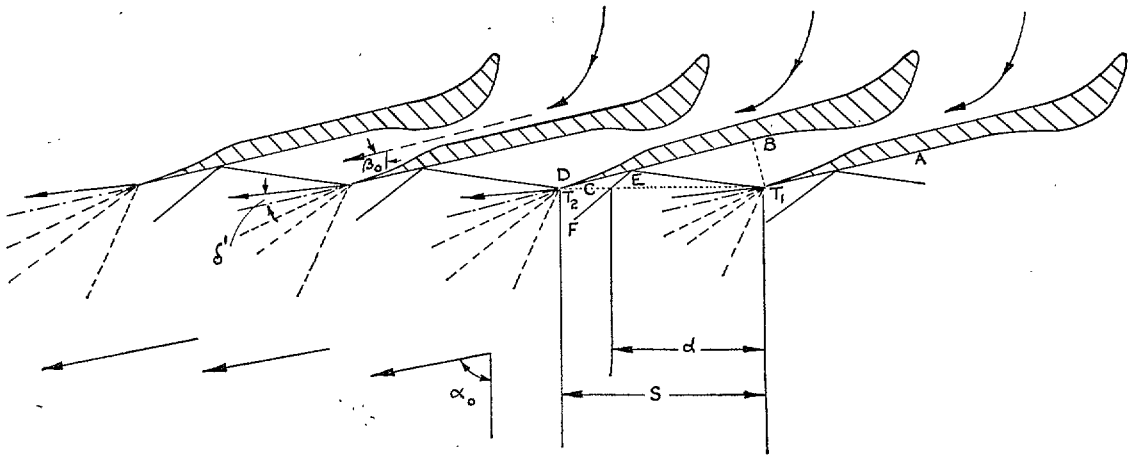

FIG. 2. A shock system causing deviation of the exit flow.

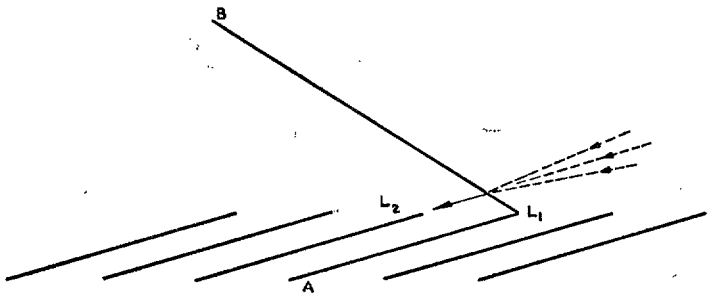

FIG. 3. Zero-thickness rotor blades operate at zero incidence.

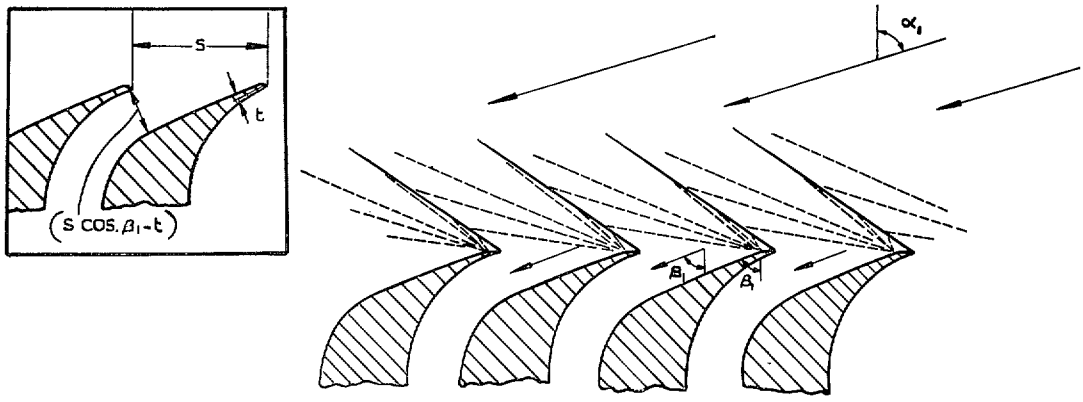

FIG. 4. Rotor blades with a leading-edge chamfer operate at a fixed positive incidence.

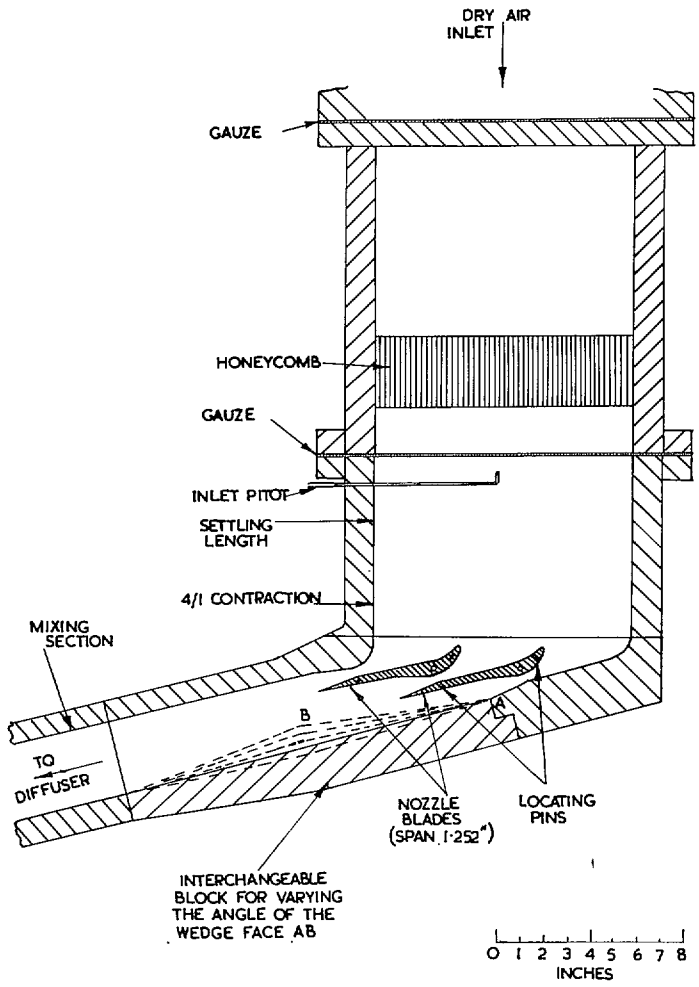

FIG. 5. Section through nozzle cascade tunnel.

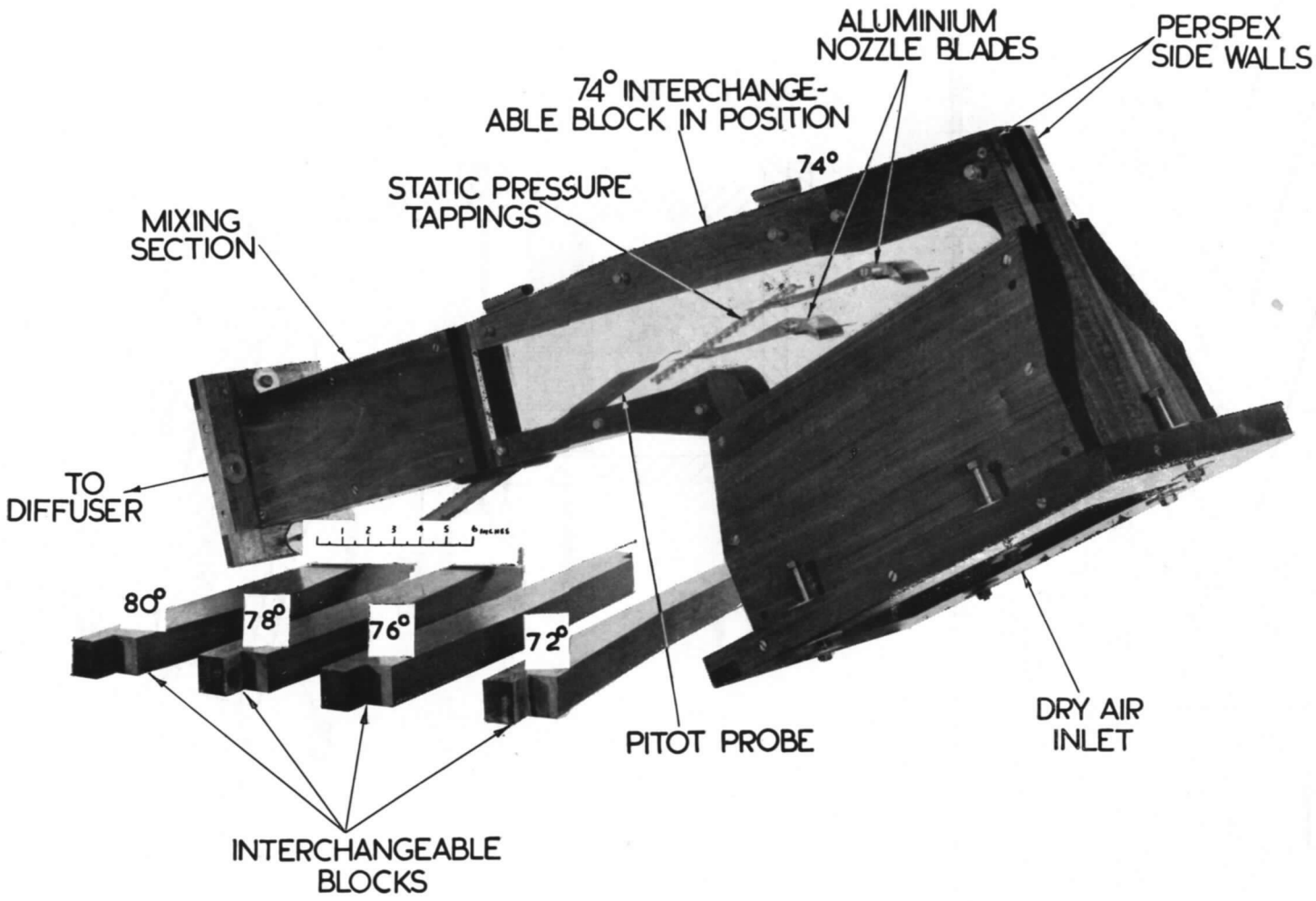

FIG. 6. Photograph of the nozzle cascade tunnel.

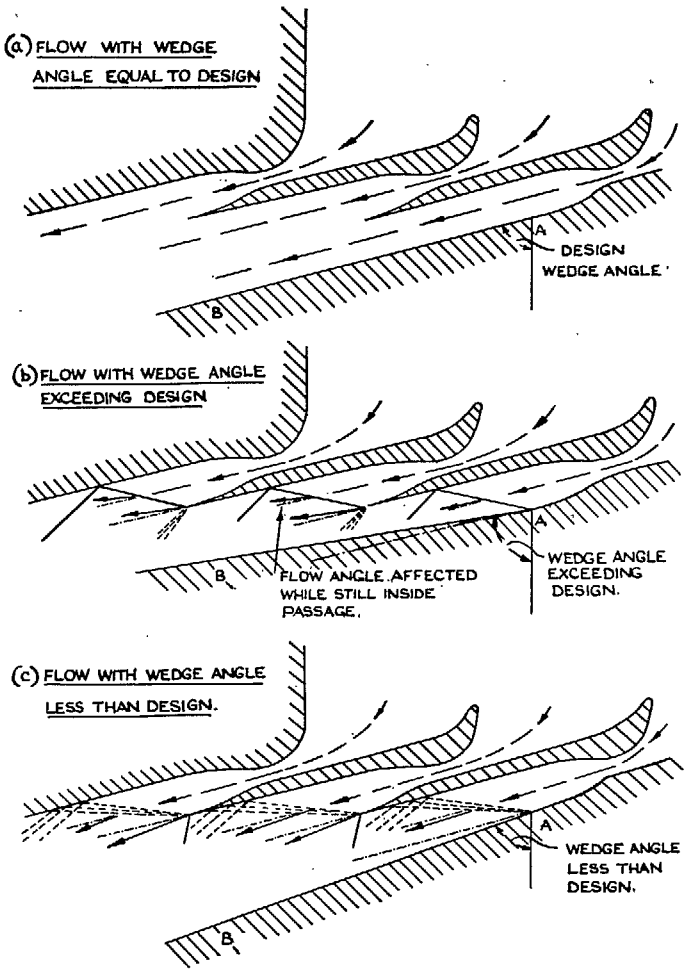

FIG. 7. Basic expectations from the tunnel. (Nozzle expansions here assumed isentropic.)

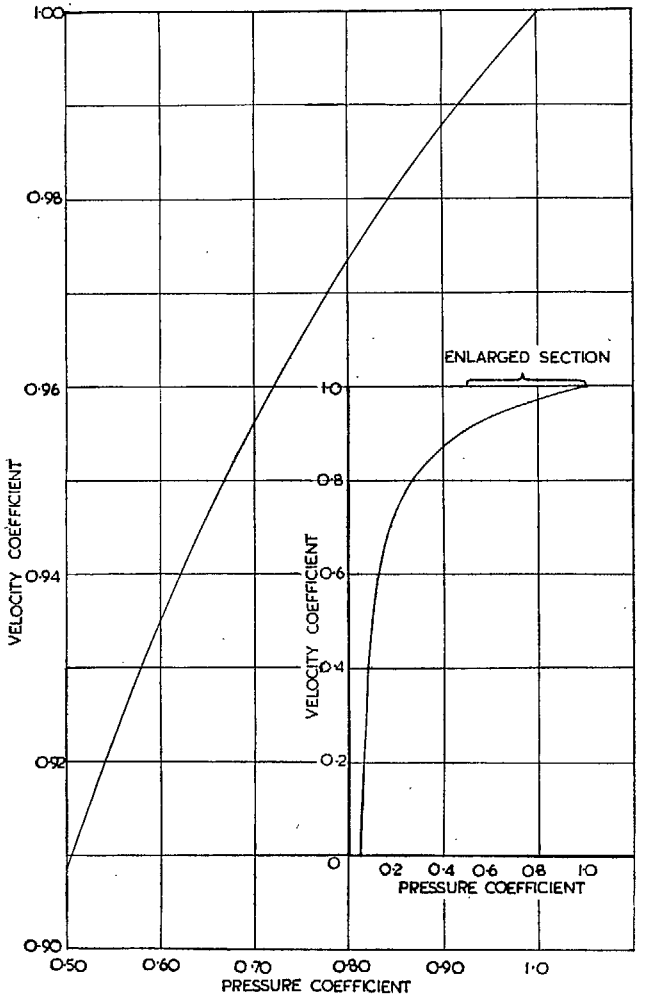

FIG. 8. The relation between velocity coefficient and pressure coefficient when the isentropic Mach number is 2·50.

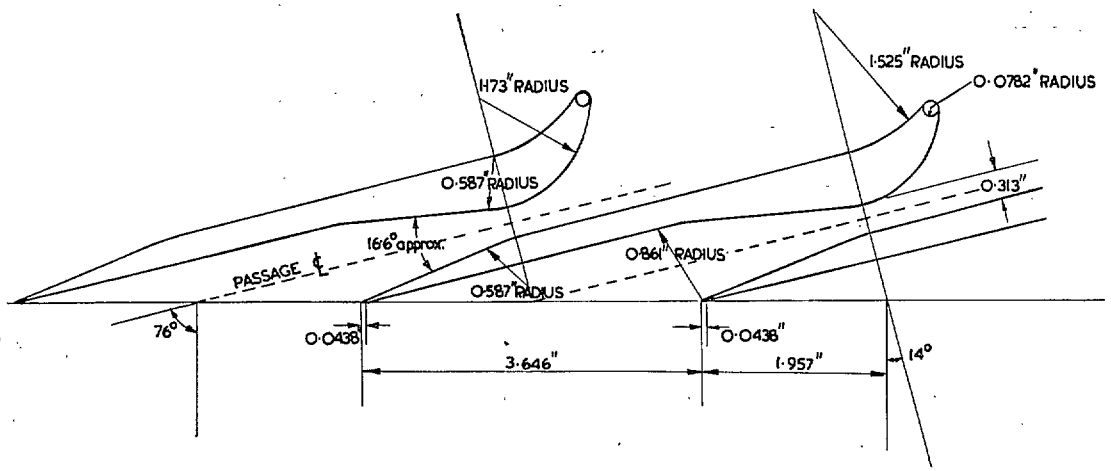

FIG. 9. The cascade design.

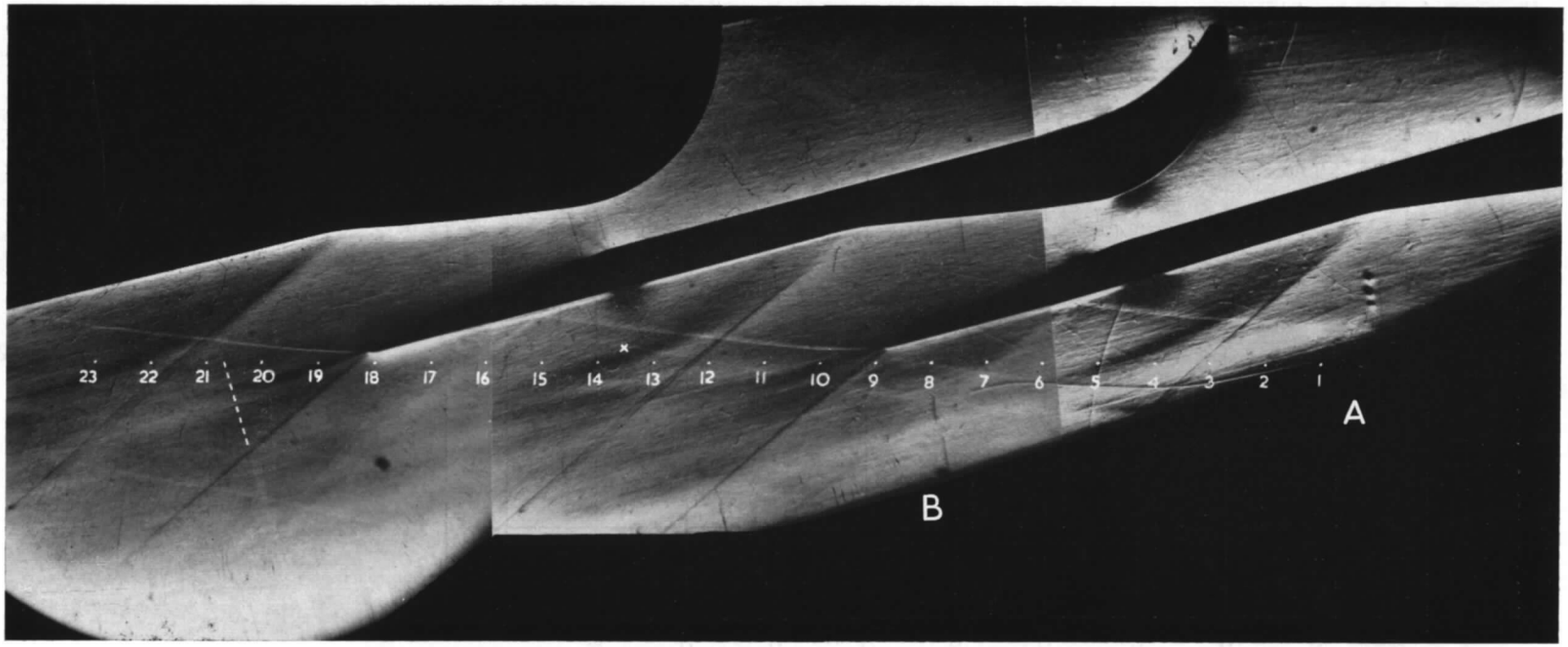

FIG. 10. Composite Schlieren photograph for the design condition (74 deg block), showing the wall static-pressure measuring positions.

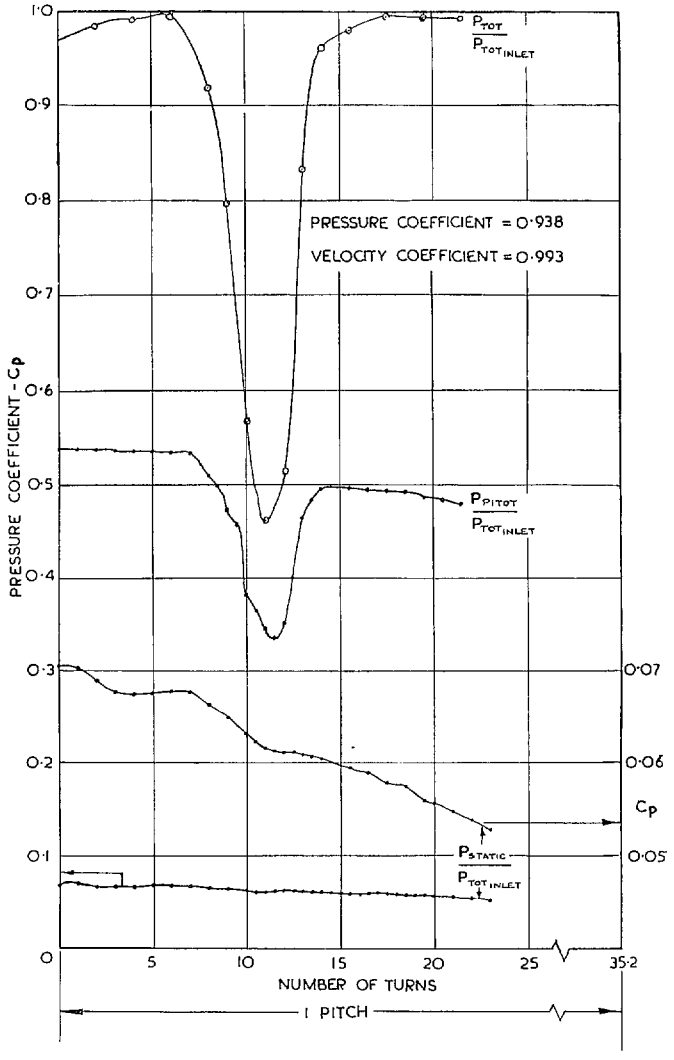

FIG. 11. A typical wake traverse at design (50 per cent span).

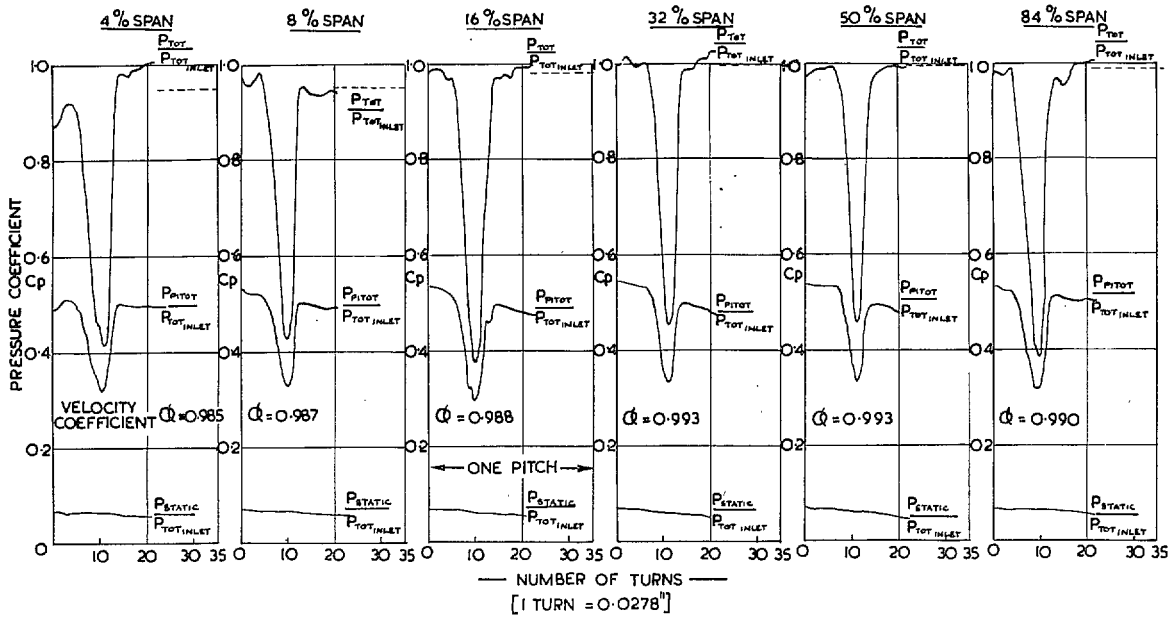

FIG. 12. Wake traverses at the six spanwise stations at design.

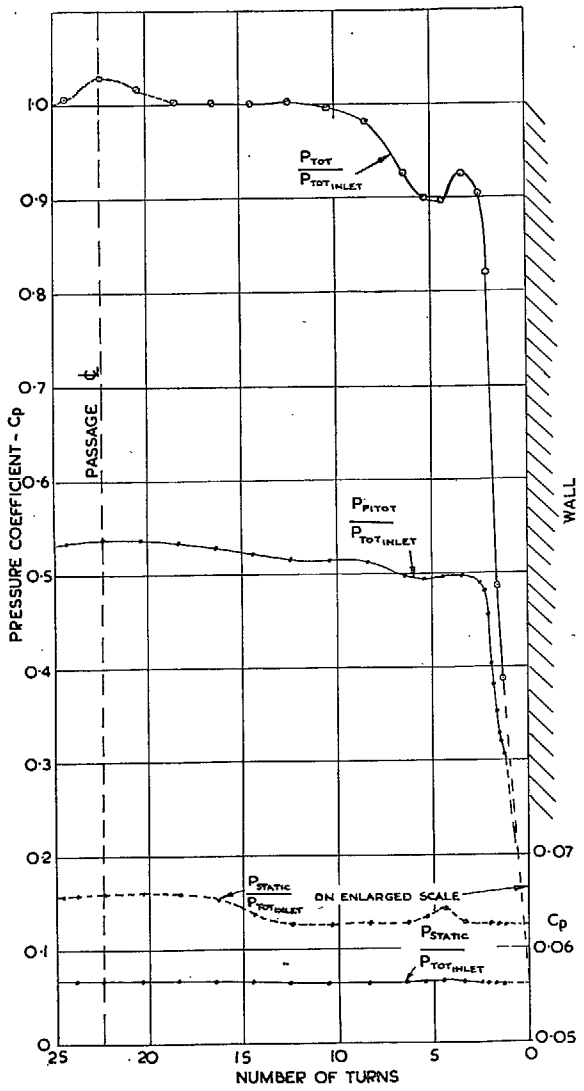

FIG. 13. The boundary-layer traverse at design.

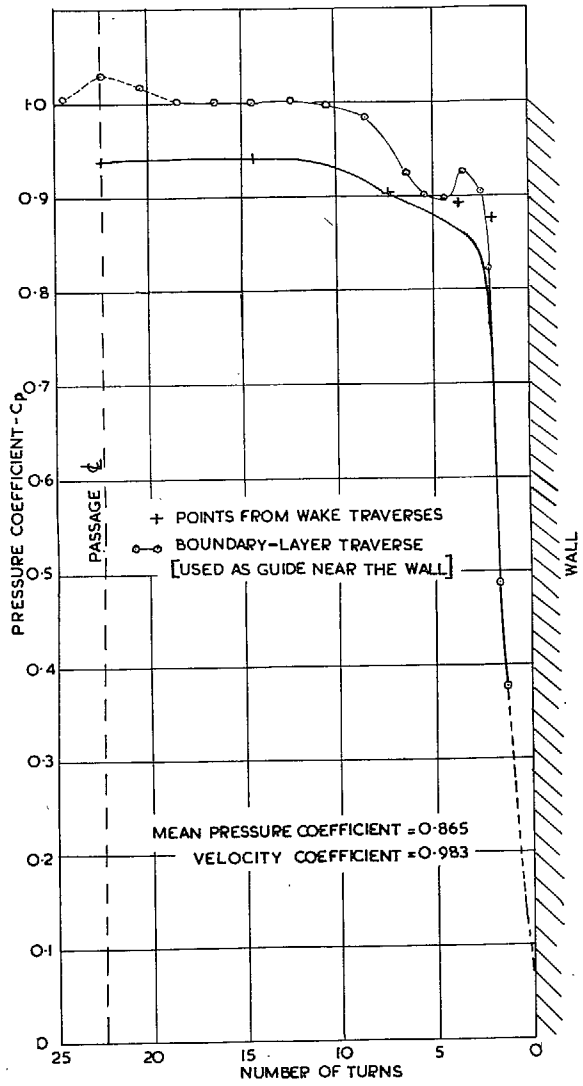

FIG. 14. The distribution of total pressure across the span at design.

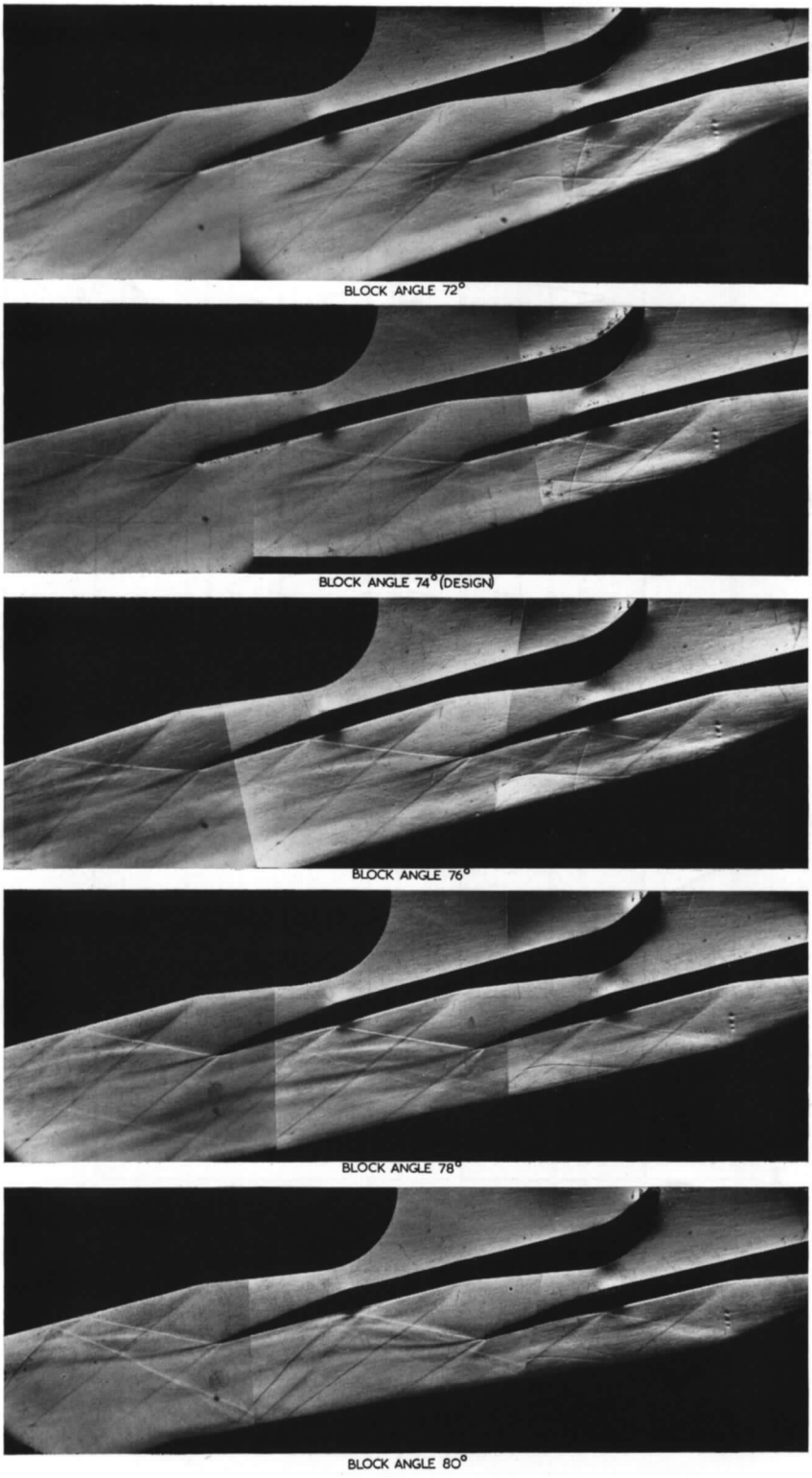

FIG. 15. Composite Schlieren photographs for a range of pressure ratios (block angles 72 to 80 deg).

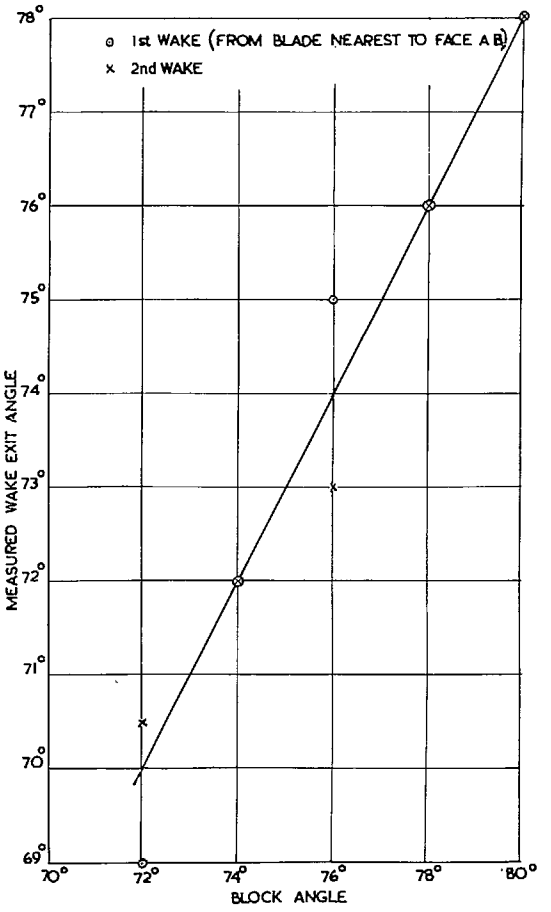

FIG. 16. Change of wake angle with block angle.

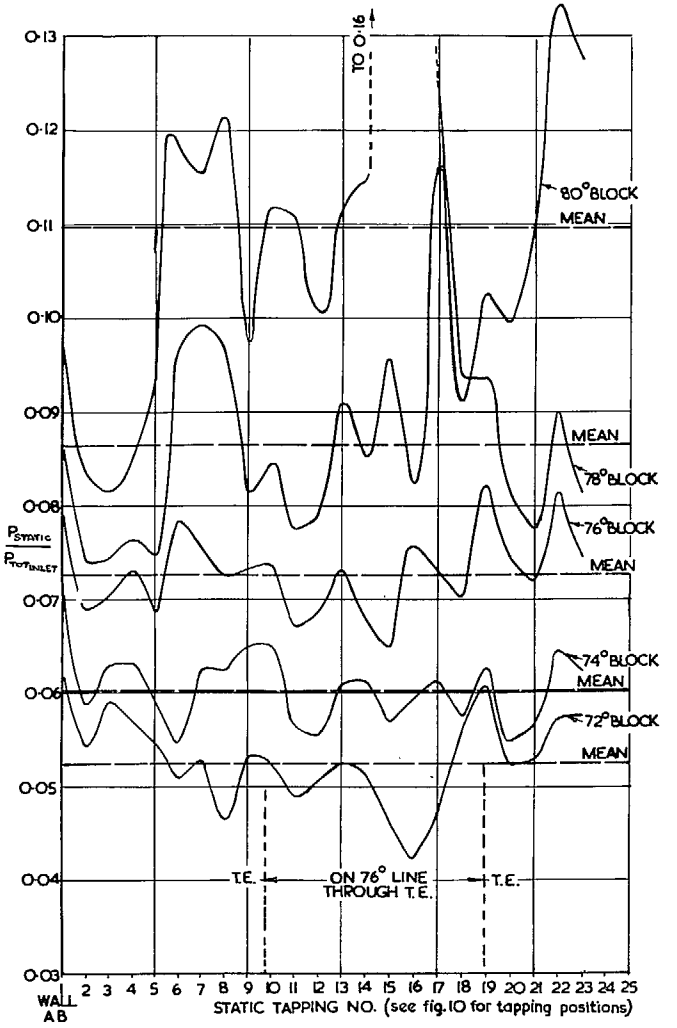

FIG. 17. Exit distributions of static pressure for a range of pressure ratios (block angles 72 to 80 deg).

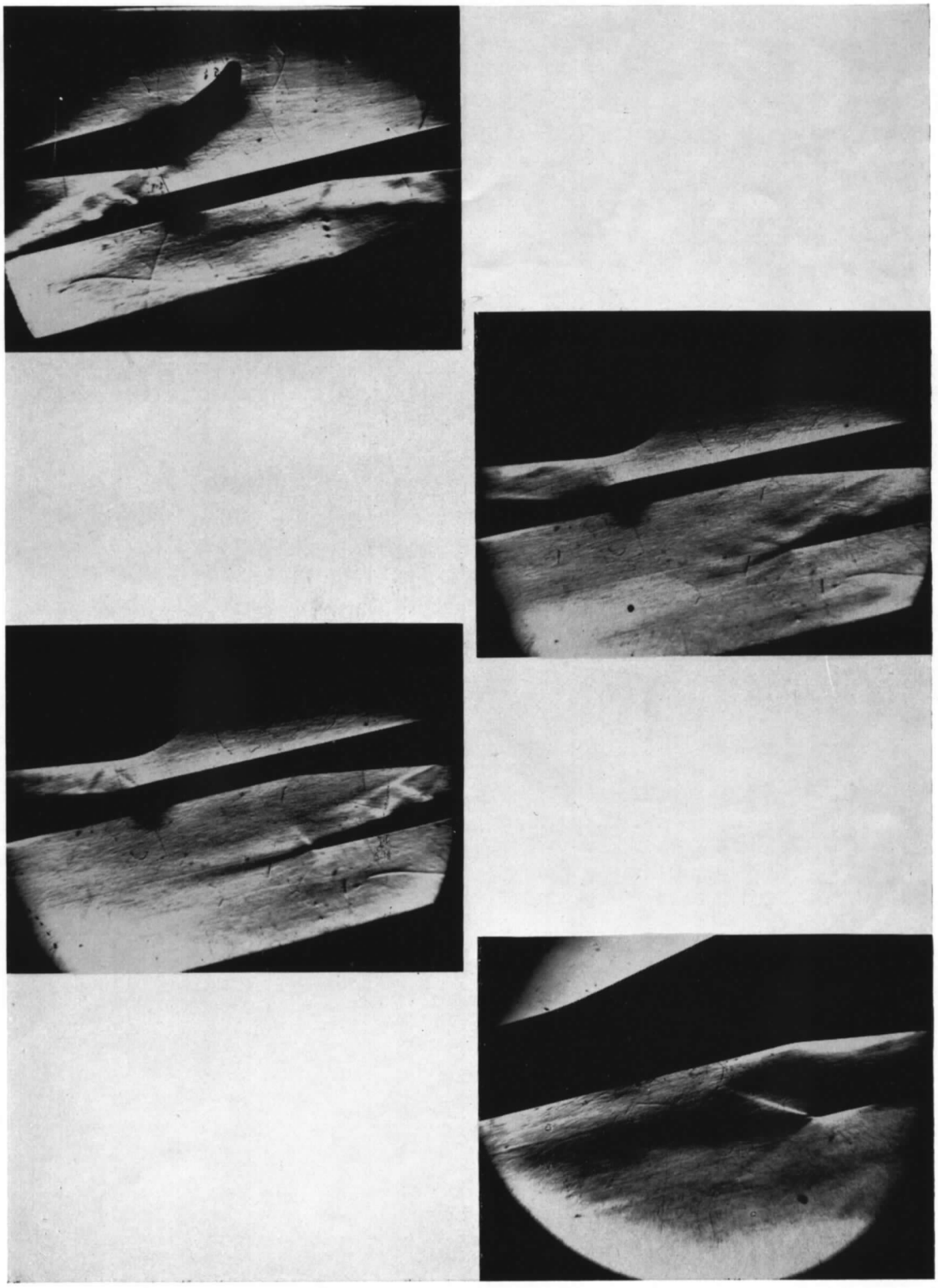

FIG. 18. Schlieren photographs with the tunnel valve partly closed—for the 74 deg block, miscellaneous positions for the valve and for the Schlieren system.

(84340) Wt. 67/1876 K.5 6/62 Hw.

Publications of the Aeronautical Research Council

ANNUAL TECHNICAL REPORTS OF THE AERONAUTICAL RESEARCH COUNCIL (BOUND VOLUMES)

1942 Vol. I. Aero and Hydrodynamics, Aerofoils, Airscrews, Engines. 75*s.* (post 2*s.* 9*d.*)
Vol. II. Noise, Parachutes, Stability and Control, Structures, Vibration, Wind Tunnels. 47*s.* 6*d.* (post 2*s.* 3*d.*)

1943 Vol. I. Aerodynamics, Aerofoils, Airscrews. 80*s.* (post 2*s.* 6*d.*)
Vol. II. Engines, Flutter, Materials, Parachutes, Performance, Stability and Control, Structures. 90*s.* (post 2*s.* 9*d.*)

1944 Vol. I. Aero and Hydrodynamics, Aerofoils, Aircraft, Airscrews, Controls. 84*s.* (post 3*s.*)
Vol. II. Flutter and Vibration, Materials, Miscellaneous, Navigation, Parachutes, Performance, Plates and Panels, Stability, Structures, Test Equipment, Wind Tunnels. 84*s.* (post 3*s.*)

1945 Vol. I. Aero and Hydrodynamics, Aerofoils. 130*s.* (post 3*s.* 6*d.*)
Vol. II. Aircraft, Airscrews, Controls. 130*s.* (post 3*s.* 6*d.*)
Vol. III. Flutter and Vibration, Instruments, Miscellaneous, Parachutes, Plates and Panels, Propulsion. 130*s.* (post 3*s.* 3*d.*)
Vol. IV. Stability, Structures, Wind Tunnels, Wind Tunnel Technique. 130*s.* (post 3*s.* 3*d.*)

1946 Vol. I. Accidents, Aerodynamics, Aerofoils and Hydrofoils. 168*s.* (post 3*s.* 9*d.*)
Vol. II. Airscrews, Cabin Cooling, Chemical Hazards, Controls, Flames, Flutter, Helicopters, Instruments and Instrumentation, Interference, Jets, Miscellaneous, Parachutes. 168*s.* (post 3*s.* 3*d.*)
Vol. III. Performance, Propulsion, Seaplanes, Stability, Structures, Wind Tunnels. 168*s.* (post 3*s.* 6*d.*)

1947 Vol. I. Aerodynamics, Aerofoils, Aircraft. 168*s.* (post 3*s.* 9*d.*)
Vol. II. Airscrews and Rotors, Controls, Flutter, Materials, Miscellaneous, Parachutes, Propulsion, Seaplanes, Stability, Structures, Take-off and Landing. 168*s.* (post 3*s.* 9*d.*)

1948 Vol. I. Aerodynamics, Aerofoils, Aircraft, Airscrews, Controls, Flutter and Vibration, Helicopters, Instruments, Propulsion, Seaplane, Stability, Structures, Wind Tunnels. 130*s.* (post 3*s.* 3*d.*)
Vol. II. Aerodynamics, Aerofoils, Aircraft, Airscrews, Controls, Flutter and Vibration, Helicopters, Instruments, Propulsion, Seaplane, Stability, Structures, Wind Tunnels. 110*s.* (post 3*s.* 3*d.*)

Special Volumes

Vol. I. Aero and Hydrodynamics, Aerofoils, Controls, Flutter, Kites, Parachutes, Performance, Propulsion, Stability. 126*s.* (post 3*s.*)
Vol. II. Aero and Hydrodynamics, Aerofoils, Airscrews, Controls, Flutter, Materials, Miscellaneous, Parachutes, Propulsion, Stability, Structures. 147*s.* (post 3*s.*)
Vol. III. Aero and Hydrodynamics, Aerofoils, Airscrews, Controls, Flutter, Kites, Miscellaneous, Parachutes, Propulsion, Seaplanes, Stability, Structures, Test Equipment. 189*s.* (post 3*s.* 9*d.*)

Reviews of the Aeronautical Research Council

1939–48 3*s.* (post 6*d.*) 1949–54 5*s.* (post 5*d.*)

Index to all Reports and Memoranda published in the Annual Technical Reports

1909–1947 R. & M. 2600 (out of print)

Indexes to the Reports and Memoranda of the Aeronautical Research Council

Between Nos. 2351–2449	R. & M. No. 2450	2*s.* (post 3*d.*)
Between Nos. 2451–2549	R. & M. No. 2550	2*s.* 6*d.* (post 3*d.*)
Between Nos. 2551–2649	R. & M. No. 2650	2*s.* 6*d.* (post 3*d.*)
Between Nos. 2651–2749	R. & M. No. 2750	2*s.* 6*d.* (post 3*d.*)
Between Nos. 2751–2849	R. & M. No. 2850	2*s.* 6*d.* (post 3*d.*)
Between Nos. 2851–2949	R. & M. No. 2950	3*s.* (post 3*d.*)
Between Nos. 2951–3049	R. & M. No. 3050	3*s.* 6*d.* (post 3*d.*)
Between Nos. 3051–3149	R. & M. No. 3150	3*s.* 6*d.* (post 3*d.*)

HER MAJESTY'S STATIONERY OFFICE

from the addresses overleaf

Printed and published by
HER MAJESTY'S STATIONERY OFFICE

To be purchased from
York House, Kingsway, London W.C.2
423 Oxford Street, London W.1
13A Castle Street, Edinburgh 2
109 St. Mary Street, Cardiff
39 King Street, Manchester 2
50 Fairfax Street, Bristol 1
35 Smallbrook, Ringway, Birmingham 5
80 Chichester Street, Belfast 1
or through any bookseller

Printed in England

S.O. Code No. 23-3273